Materials Research Proceedings 41 (2024) 1224-1230 https://doi.org/10.21741/9781644903131-136

Enhanced formability in two-step forming for AA7075 sheet in -T6 and -W tempers

HA Jinjin[1,a *], CHOI Yumi[2,b], LEE Myoung-Gyu[2,c], and KORKOLIS Yannis P.[3,d]

[1]University of New Hampshire, Mechanical Engineering, Durham, NH 03824, USA

[2]Seoul National University, Materials Science and Engineering, Seoul 08826, Korea

[3]TU Dortmund University, Institut für Umformtechnik und Leichtbau, Dortmund 44227, Germany

[a] jinjin.ha@unh.edu, [b]yumichoi@snu.ac.kr, [c]myounglee@snu.ac.kr, [d]yannis.korkolis@iul.tu-dortmund.de

Keywords: Formability, Multi-Step Forming, Aa7075, Hole Expansion, Anisotropy

Abstract. In response to stringent environmental regulations, the automotive industry is increasingly prioritizing lightweighting, prompting a shift towards high-strength aluminum alloys while the low formability of these alloys remain a limiting factor. This study explores a solution through a two-step forming process applied to AA7075 sheets utilizing -T6 and -W tempers. Firstly, two-step uniaxial tension experiments are performed at two prestraining levels in the -T6 temper followed by subsequent tensions in the -W. Both cases exhibit significant plastic deformation before fracture, overcoming the thinning accumulated in the first step. Additionally, a two-step hole expansion experiment is conducted under the same tempering conditions. Results are compared with single operations in each temper, evaluating force-displacement curves and thickness strain distribution around the hole. The study highlights the substantial contribution to formability enhancement, demonstrating 80% higher cup height and twice greater thinning to fracture compared to conventional single-step operations.

Introduction

The auto industry's focus on lightweighting, driven by environmental concerns, has escalated the demand for aluminum alloys, particularly the high-strength 6xxx and 7xxx series, as substitutes for steel components. However, their limited ductility requires technical interventions, such as forming at elevated temperatures or specific tempering conditions, to enhance formability. Tackling these formability challenges is crucial for advancing environmentally conscious and efficient automotive solutions, necessitating innovative approaches and tailored processes within the industry [1–3].

One metric to evaluate the stretch flange formability is expanding of a circular hole in a sheet sample [4,5]. In the hole expansion experiment, the free edge of the hole is stretched uniaxially along a circumferential direction but the compatibility with surrounding materials enables larger deformation near the edge than in a simple uniaxial tension test [4,6]. As a result, the simple uniaxial tension experiment always underestimates a formability limit, which represents an inappropriateness as an evaluation method for the stretch flange formability.

In this paper, the formability improvement in two-step forming is investigated by utilizing benefits of different tempering conditions in AA7075 aluminum sheet. Two experiments of each uniaxial tension and hole expansion in two-step operation are performed with combination of -T6 and -W tempers and the results are compared with single operation of individual tempers. The comparison shows significant improvement of formability in two-step forming with two tempers.

Material characterization in uniaxial tension

Mechanical property of AA7075 in -T6 (UT_{T6}) and -W (UT_W) is characterized by uniaxial tension experiment in 0°, 45°, and 90° from the rolling direction (RD). The material is received in -T6 and

then heat treated to alter the temper to -W as shown in Fig. 1 [7]. The timing is rigorously maintained for a duration of 15 minutes, as the -W temper condition is temporary and highly time sensitive, and significant changes in mechanical properties can occur after a certain time. A constant crosshead velocity of 3.6 mm/min is applied in the both monotonic and two-step uniaxial tension experiments, inducing the strain rate of ~10^{-3}/s, assuming the deformation is uniform in the gauge area for both tempers.

The stress-strain curves from monotonic uniaxial tension under each temper are depicted in Fig. 2a [8]. UT_{T6} in the RD exhibits the highest yield stress at approximately 530 MPa and ultimate tensile strength around 590 MPa. However, its uniform elongation is only 10%, presenting a challenge in terms of formability. In contrast, UT_W in the RD displays significantly lower flow stress than UT_{T6}, e.g., yield stress around 165 MPa, but demonstrates greater ductility until fracture, signifying a meaningful improvement in formability under uniaxial tension in the -W temper. It's noteworthy that the engineering stress and strain of UT_W are calculated without considering deformation heterogeneity in the gauge region caused by Portevin-Le Chatelier (PLC) bands [9]. Additionally, plastic anisotropy in r-value, an indicator of thinning resistance during uniaxial tension deformation, is compared in Fig. 2b. The values are highest at 45° and lowest in the RD in both tempers, and the temper-based difference is minor. Thus, under the given conditions, plastic anisotropy in r-value is more pronounced than in flow stress for both tempers, highlighting the greater influence of temper changes on stress-strain behavior than on r-value.

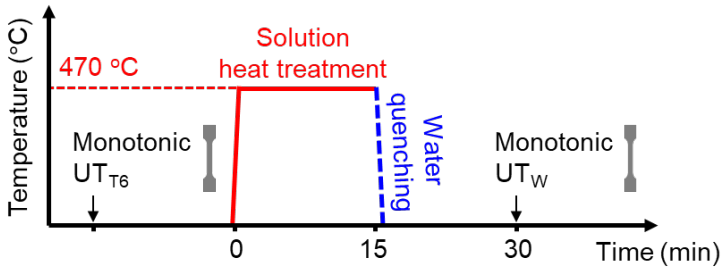

Figure 1. Heat treatment for monotonic uniaxial tension in -W temper

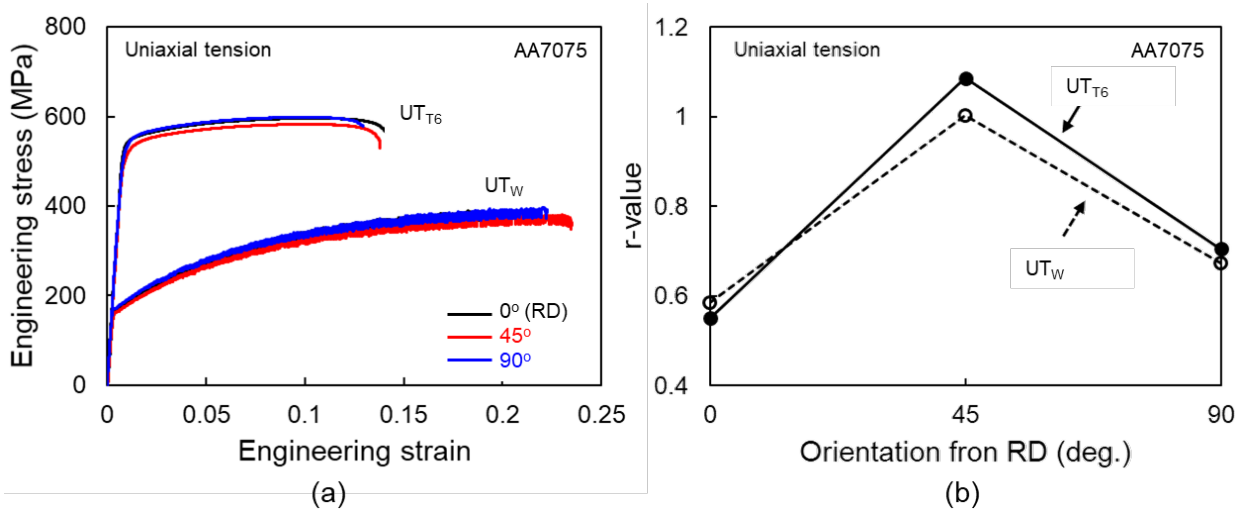

Figure 2. Mechanical properties of the AA7075 in -T6 (UT_{T6}) and –W (UT_W): (a) engineering stress-strain curves and (b) r-values in the three orientations

Two-step uniaxial tension

To evaluate formability improvement with -T6 and -W tempers, two-step uniaxial tension experiment is first performed with different prestraining and investigates the effect of prior deformation on the heat treatment and subsequent loading. ASTM E8 specimen in -T6 is stretched

with two grip displacements δ_{UT_1}=5 mm and δ_{UT_1}=8 mm in the first step ($UT_{1,T6}$), and then unloaded for the solution heat treatment to -W temper. After 15 minutes of holding in air, the subsequent uniaxial tension in -W ($UT_{2,W}$) is performed until the fracture. The schematic is shown in Fig. 3.

Figure 4 shows the engineering stress-strain curves of two-step uniaxial tension experiments. Two prestraining levels applied by δ_{UT_1}=5 mm and δ_{UT_1}=8 mm in the $UT_{1,T6}$ are led to different conditions: δ_{UT_1}=5 mm produces uniform deformation of 0.073 true strain in average while δ_{UT_1}=8 mm triggers the diffused necking with varying true strain range from 0.1 to 0.12 as shown in the strain field measured by stereo-type digital image correlation (DIC) system. Nevertheless, the both engineering stress-strain curves of $UT_{2,W}$ can reach significant deformation until the fracture and even $UT_{2,W}$ with δ_{UT_1}=5 mm shows the negligible ductility loss compared to the monotonic UT_W.

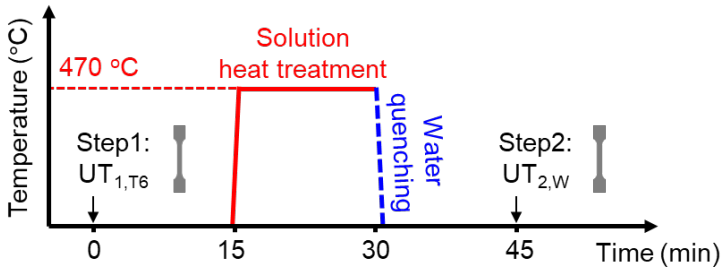

Figure 3. Schematic for two-step uniaxial tension in -T6 ($UT_{1,T6}$) and -W ($UT_{2,W}$) tempers

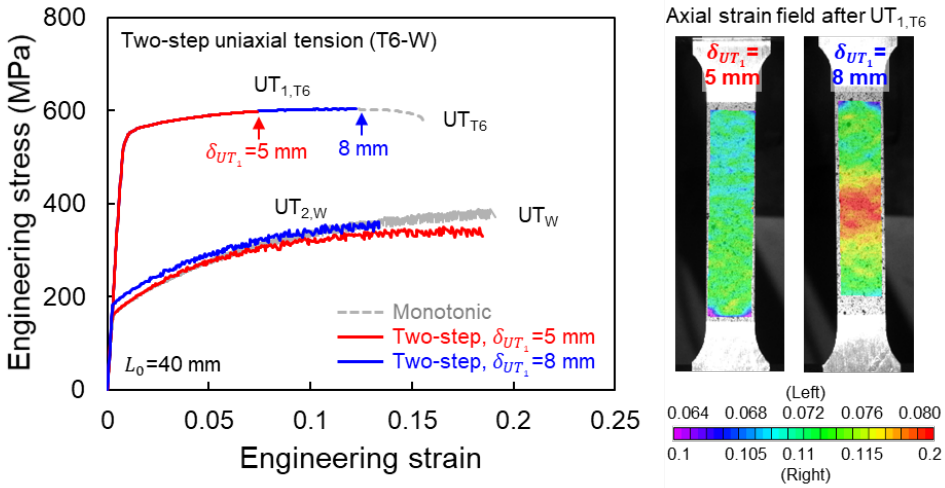

Figure 4. Engineering stress-strain curves of monotonic (gray dashed) in -T6 and -W tempers and two-step uniaxial tensions (red and blue solid) of δ_{UT_1}=5 and 8 mm and the axial strain fields

Two-step hole expansion

In addition to the two-step uniaxial tension, two-step hole expansion experiment is performed with the same heat treatment and prestraining approach with the two-step uniaxial tension as in Fig. 5. A double-action hydraulic Greenerd press in Fig. 6 is used with the stereo-type DIC system to capture the surface strain field [10,11]. A square specimen with a circular hole of 17.5 mm diameter is prepared by end-milling for the best surface quality especially for the hole edge. The punch face at the contact with a blank is lubricated using diluted Drawsol. A constant punch velocity of ~21 mm/min is applied in the hole expansion experiments for both tempers, assuming

the average strain rate in the hole periphery is ~10^{-3}/s with ignoring the deformation heterogeneity due to anisotropy and PLC bands.

The initial hole expansion in -T6 temper ($HE_{1,T6}$) involves a punch displacement of δ_{HE_1}=13 mm, yielding a prestraining level similar to $UT_{1,T6}$ with δ_{UT_1}=8 mm in two-step uniaxial tension (see right figure in Fig. 7a for the circumferential strain field in $HE_{1,T6}$). Following identical heat treatment and holding time, the subsequent hole expansion is conducted in -W temper ($HE_{2,W}$) until the fracture. The punch force-displacement curves in Fig. 7a shows significant increase of punch displacement at the onset of fracture in two-step hole expansion compared to the single operation at each temper (HE_{T6} and HE_W, respectively). Notably, the total enhancement in two-step hole expansion, in terms of punch displacement at fracture, is nearly 80% compared to the lowest case in HE_{T6}, evidently surpassing HE_W as well.

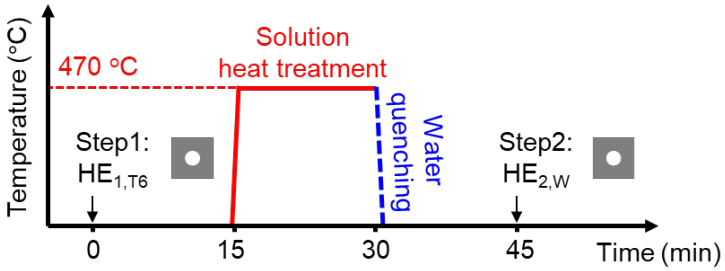

Figure 5. Schematic for two-step hole expansion in -T6 ($HE_{1,T6}$) and -W ($HE_{2,W}$) tempers

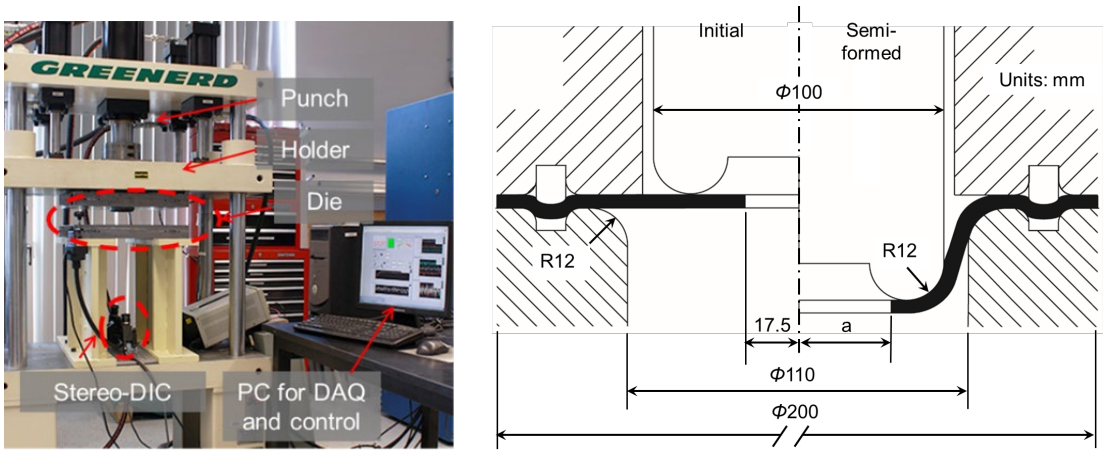

(a) (b)

Figure 6. Experimental setup for hole expansion: (a) machine and equipment and (b) tools

Figure 8 shows the thickness strain variations around the hole in $HE_{1,T6}$ after prestraining with δ_{HE_1}=13 mm and in the $HE_{2,W}$ at the onset of fracture in comparison of single operation HE_{T6} and HE_W. The strain is measured by the stereo-type DIC system along a hoop with initial radius of 20 mm and the extracted data is plotted with respect to the angle from the RD. As seen in Fig. 7, two-step hole expansion can reach to the highest level of thinning at the onset of fracture in the second step compared to the single operations HE_{T6} and HE_W. It should be noted that the prestraining $HE_{1,T6}$ is factored into the calculation of the thickness strain in $HE_{2,W}$, which is crucial to account for the cumulative deformation experienced throughout the entire process. Interestingly, the maximum thinning locations remain consistent along the RD, i.e., at 180°, regardless the temper conditions. This represents the heat treatment to alter the temper from -T6 to -W does not influence

the plastic anisotropy in the current experimental conditions while it can significantly lower the force-displacement curve. This is the same result seen in Fig. 2.

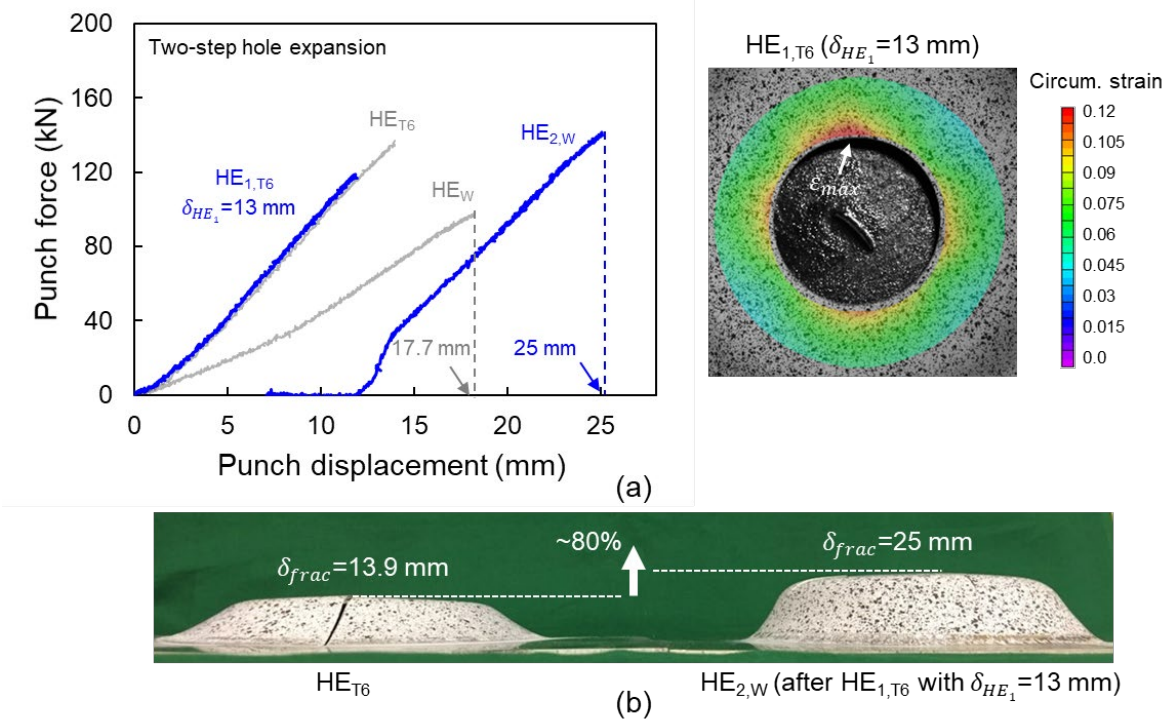

Figure 7. Formability enhancement in two-step hole expansion: (a) punch force-displacement curves of two-step ($HE_{1,T6}$ and $HE_{2,W}$) and single operation (HE_{T6} and HE_W) with the circumferential strain field after prestraining in $HE_{1,T6}$ with δ_{HE_1}=13 mm and (b) specimens side view to compare the height at fracture in the lowest (HE_{T6}) and the highest (two-step: $HE_{1,T6}$ followed by $HE_{2,W}$) cases

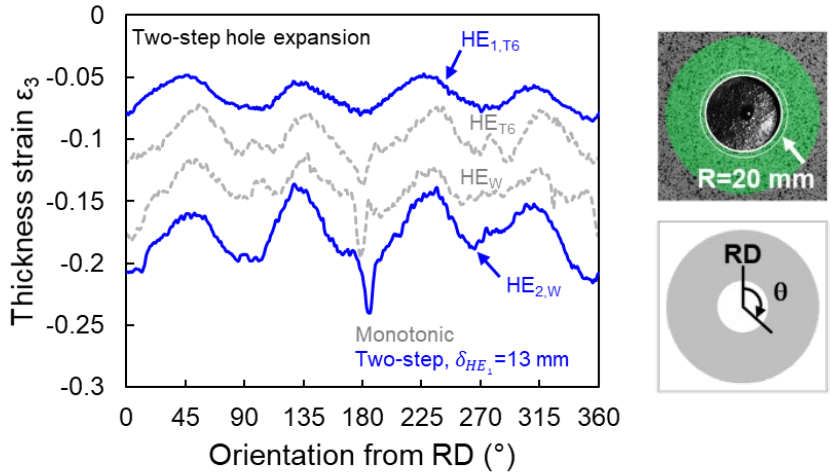

Figure 8. Thickness strain variation along the angle from the RD measured from a hoop with an initial radius of 20 mm

Summary and conclusion

This study investigates the formability improvement through a two-step forming approach, leveraging the advantages of different tempering conditions in AA7075 aluminum sheets. Two-

step uniaxial tension and two-step hole expansion experiments are conducted, combining -T6 and -W tempers, with results compared to single operations under each temper. The key findings are as follows:

- Formability is significantly improved in two-step forming with both -T6 and -W tempers. This underscores the efficacy of the two-step forming strategy to exploit the exiting formability in -T6 and to maximize the overall formability through the additional deformation in -W temper.
- Heat treatment during two-step forming alters the temper from -T6 and –W, reducing flow stress in subsequent deformation without affecting the plastic anisotropy in the current experiment. Consequently, the maximum thinning location in the hole expansion remains consistent in the RD leading to the initial rupture.

Acknowledgement
This research was partially supported by the US National Science Foundation (NSF) under awards 1563216 and 1929873. JH appreciates the support from Alexander von Humboldt fellowship for experienced researcher and C. Dunn for the help to operate the hydraulic press machine. Start-up funds at The Ohio State University are acknowledged for contributing to the visit of YC. YC appreciates partial support from National Research Foundation of Korea (NRF-2012R1A5A1048294). The material is supplied by MS-Autotech.

References

[1] O.N. Senkov, M.R. Shagiev, S. V. Senkova, D.B. Miracle, Precipitation of Al3(Sc,Zr) particles in an Al-Zn-Mg-Cu-Sc-Zr alloy during conventional solution heat treatment and its effect on tensile properties, Acta Materialia 56 (2008) 3723–3738. https://doi.org/10.1016/j.actamat.2008.04.005

[2] E. Sáenz de Argandoña, L. Galdos, R. Ortubay, J. Mendiguren, X. Agirretxe, Room Temperature Forming of AA7075 Aluminum Alloys: W-Temper Process, Key Engineering Materials 651–653 (2015) 199–204. https://doi.org/10.4028/www.scientific.net/kem.651-653.199

[3] Y. Choi, J. Lee, S.S. Panicker, H.-K. Jin, S.K. Panda, M.-G. Lee, Mechanical properties, springback, and formability of W-temper and peak aged 7075 aluminum alloy sheets: Experiments and modeling, Int J Mech Sci 170 (2020) 105344. https://doi.org/10.1016/J.IJMECSCI.2019.105344

[4] A. Parmar, P.B. Mellor, Plastic expansion of a circular hole in sheet metal subjected to biaxial tensile stress, Int J Mech Sci 20 (1978) 707–720. https://doi.org/10.1016/0020-7403(78)90057-7

[5] T. Kuwabara, K. Hashimoto, E. Iizuka, J.W. Yoon, Effect of anisotropic yield functions on the accuracy of hole expansion simulations, Journal of Materials Processing Technology 211 (2011) 475–481. https://doi.org/10.1016/j.jmatprotec.2010.10.025

[6] J.Y. Lee, K.J. Lee, M.G. Lee, T. Kuwabara, F. Barlat, Numerical modeling for accurate prediction of strain localization in hole expansion of a steel sheet, Int J Solids Struct 156–157 (2019) 107–118. https://doi.org/10.1016/j.ijsolstr.2018.08.005

[7] E. Sáenz de Argandoña, L. Galdos, R. Ortubay, J. Mendiguren, X. Agirretxe, Room Temperature Forming of AA7075 Aluminum Alloys: W-Temper Process, Key Engineering Materials (2015). https://doi.org/10.4028/www.scientific.net/kem.651-653.199

[8] Y. Choi, J. Ha, M.G. Lee, Y.P. Korkolis, Effect of plastic anisotropy and Portevin-Le Chatelier bands on hole-expansion in AA7075 sheets in -T6 and -W tempers, J Mater Process Technol 296 (2021) 117211. https://doi.org/10.1016/J.JMATPROTEC.2021.117211

[9] Y. Choi, J. Ha, M.G. Lee, Y.P. Korkolis, Observation of Portevin-le Chatelier effect in aluminum alloy 7075-w under a heterogeneous stress field, Scr Mater 205 (2021) 114178. https://doi.org/10.1016/J.SCRIPTAMAT.2021.114178

[10] J. Ha, S. Coppieters, Y.P. Korkolis, on the Expansion of a Circular Hole in an Orthotropic Elastoplastic Thin Sheet, International Journal of Mechanical Sciences (2020) 105706. https://doi.org/10.1016/j.ijmecsci.2020.105706

[11] Y.P. Korkolis, B. Brownell, S. Coppieters, H. Tian, Modeling of hole-expansion of AA6022-T4 aluminum sheets with anisotropic non-quadratic yield functions, Journal of Physics: Conference Series 734 (2016). https://doi.org/10.1088/1742-6596/734/3/032083